Generalized dimensions of laser attractors

U. Hübner, W. Klische, and C. O. Weiss
Physikalisch-Technische Bundesanstalt, Braunschweig, Germany
(Received 12 July 1991)

We use generalized dimensions to compare the dynamics of an optically pumped NH_3 ring laser with that of the Lorenz model. While for pure single-mode emission we find excellent agreement between dimension spectra of the laser and the Lorenz attractor, for conditions of existence of a second counterpropagating mode, dimensions are found to be higher. Thus the dimension spectra reflect the larger phase space occupied by the attractor. As a further result of that comparison, we find that the frequently used correlation dimension D_2 as an estimate for the Hausdorff dimension D_0 can differ substantially from D_0, and shows little sensitivity to attractor changes.

PACS number(s): 42.50.Lc, 05.45.+b

Recently we found that the intensity dynamics of a NH_3 ring laser represent the dynamics of the Lorenz model [1] in detail [2]. Among others we compared the correlation dimension D_2 of the laser attractor with that of the Lorenz model. Reliable dimension calculations have been possible because the pulsing of the far-infrared NH_3 ring laser can be measured with a signal-to-noise ratio of about 300. Good agreement in the correlation dimension D_2 has been found. But the comparison of two attractors by just one scalar quantity is evidently not too meaningful.

This Brief Report shows a comparison of the dimension spectra of numerically calculated Lorenz chaos data, experimental Lorenz-like chaos data of a ring laser with one active propagation direction, and experimental data which obviously were influenced by a second counterpropagating mode.

As has been pointed out in [3] the geometrical and probabilistic features of strange attractors can be characterized by the Renyi dimensions D_q with any $q \geq 0$, not necessarily integer. Pawelzik and Schuster [4] generalized the correlation integral method of Grassberger and Procaccia [5] to calculate the D_q's via the generalized correlation integral

$$C^q(r)=\left[\frac{1}{N}\sum_i\left[\frac{1}{N}\sum_j\Theta(r-|\mathbf{X}_i-\mathbf{X}_j|)\right]^{q-1}\right]^{1/q-1}, \tag{1}$$

where r denotes the radius of a ball, $\mathbf{X}_i$ and $\mathbf{X}_j$ denote vectors in an embedding phase space, and N is the number of points available. The D_q's are then calculated with

$$D_q=\lim_{r\to 0}\left[\frac{1}{\ln(r)}\ln[C^q(r)]\right], \tag{2}$$

and they reflect the density distribution of points on the attractors.

In particular D_0 is the Hausdorff (or fractal) dimension, D_1 is called the information dimension, and D_2 is the correlation dimension with the relation $D_0 > D_1 > D_2 > \ldots$ so that D_2 is only a lower bound for D_0.

We have used intensity data from an 81.5-μm $^{14}NH_3$ cw far-infrared (FIR) laser [2] to calculate the D_q values from $q=0$ to 15, and to compare the D_q's with those of the squared field values (u^2 in [2]) numerically generated by integration of the Lorenz equations, with parameters $r=15$, $b=0.25$, and $s=2$ as appropriate for the laser sys-

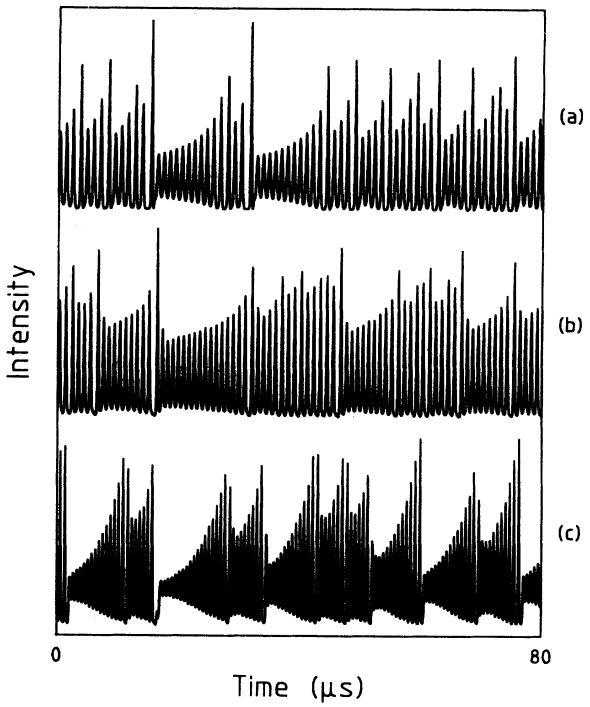

FIG. 1. Spiral-type pulsing of the laser intensity. Two thousand samples were plotted per trace. Trace (a) shows the numerically calculated Lorenz-model data. The most Lorenz-like experimental data set No. 3 is shown in trace (b), and trace (c) shows the case where obviously a second counterpropagating mode existed. Information about the experimental parameters (pressure etc.) can be found in [2].

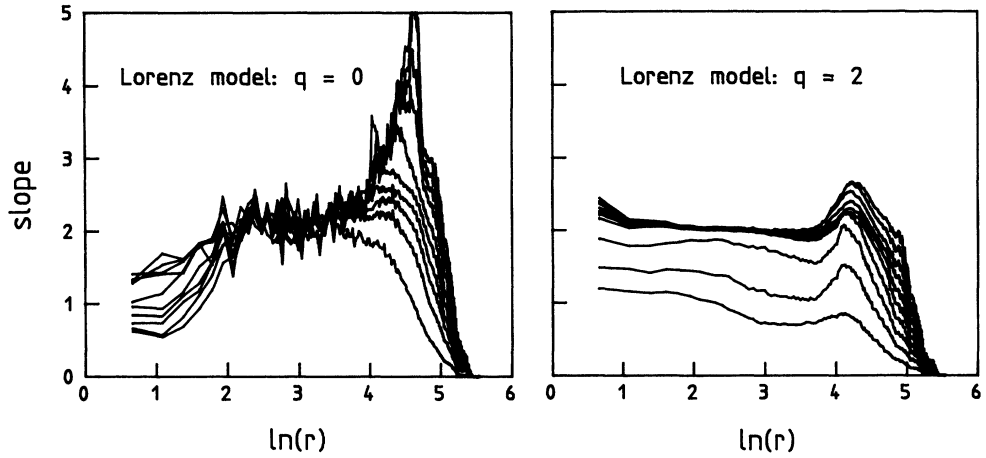

FIG. 2. Slopes $d[\ln(C_q)]/d[\ln(r)]$ of the correlation integral vs $\ln(r)$ for the case of the Lorenz model. The dimension of the embedding phase space was varied from 2 to 20 in steps in 2.

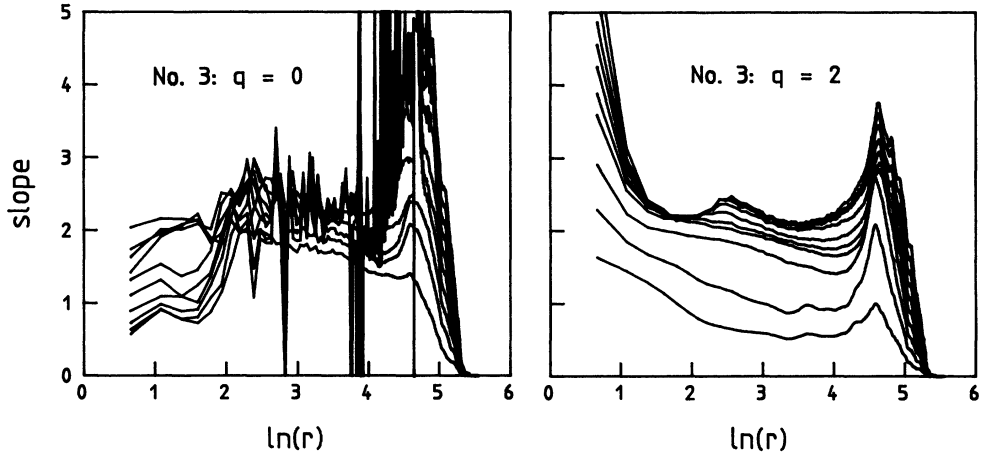

FIG. 3. Slopes as in Fig. 2 for the experimental data set No. 3 with behavior closest to the numerically calculated Lorenz-model data.

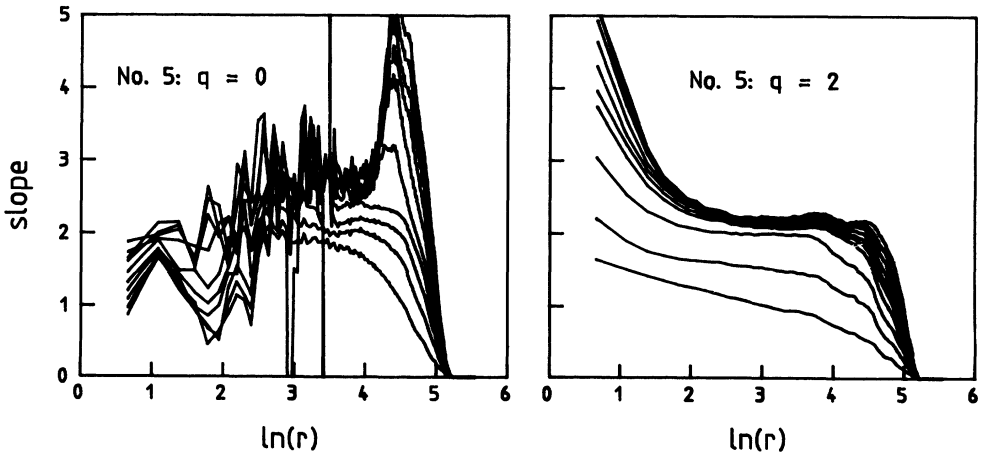

FIG. 4. Slopes as in Fig. 2 for the experimental data set No. 5 with a counterpropagating mode.

tem [2].

Twenty-six measured data sets were available. Each data set consisted of 25 000 8-bit data of laser intensity, sampled every 40 ns, with 15 to 25 samples per average chaotic pulsing period. From those data sets Fig. 1 contains No. 3 and No. 5 as representative. Number 3 proved to be the data set with behavior closest to the numerically calculated Lorenz model data set [2], and No. 5 stands for the case with a counterpropagating mode.

The procedure to calculate the correlation integrals from (1) was similar to that in [2]. Again we used the maximum norm in (1) and the time delay $\tau=n\Delta t$ (n, integer; Δt, sampling time) was chosen to be about $\frac{1}{7}$ of the averaging pulsing period. The "embedding dimension" E was varied between 2 and 20 in steps of 2 and each D_q was then calculated as an average of the last four D_q values.

Examples of the slopes $d[\ln(C_q)]/d[\ln(r)]$ of the correlation integral from which the D_q values are obtained are shown in Figs. 2–4. We find the D_q's at low q values less reliable because they put weight on the regions of low point density. In spite of the large noise of the slope curves for $q=0$, one can see that the average slope in the plateau region of data set No. 5 is significantly higher than that of No. 3 or that of the numerical Lorenz-model data.

Figure 5 shows the D_q values of the three data sets discussed. The calculated D_q values are marked with centered octagons, triangles, and crosses. To get a clear impression of the differences between the three data sets we also added an interpolation curve for each data set.

The similarity of the D_q values of data set No. 3 and the Lorenz model is obvious. The D_q values differ by about 3%, indicating an excellent agreement between the structure of the laser attractor and the Lorenz attractor. On the other hand, data set No. 5 shows significantly higher D_q values than those of the Lorenz model. In particular, the dimension D_0, which is the fractal dimension, is almost 50% higher than in the Lorenz case.

One notes that the pulsing of data set No. 5 [Fig. 1(c)], from which we calculated the D_q values of Fig. 5, differs qualitatively from the Lorenz-like case of Fig. 1(b). In particular the pulses of each spiral begin close to the steady-state laser emission and the large pulses at the end of the spirals are missing.

We have recently found [6] that the type of pulsing in Fig. 1(c) is not described by the Lorenz equations. In fact we found that the type of pulsing shown in Fig. 1(c) is associated with temporary emission of the ring laser in the opposite direction. We found that in cases such as Fig. 1(c) at the end of the spiral a small single pulse may be emitted into the opposite direction of the ring emission while the original emission is near zero. Then the inversion which is shared by the two emission directions is reduced so that the large pulses at the end of the spirals are suppressed. Additionally, the laser gain is reduced so that the next spiral starts close to the steady-state emission.

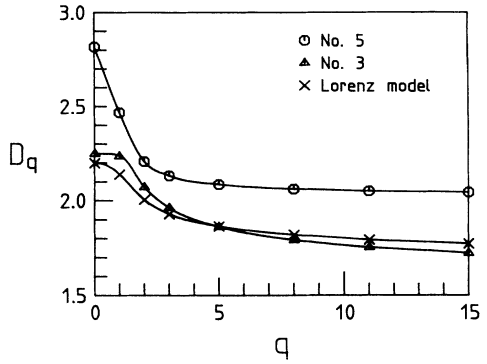

FIG. 5. Plot of the calculated D_q values (marked points) vs q for the numerically calculated Lorenz-model data set, and the experimental data sets No. 3 and No. 5. The smooth interpolation curves through the calculated and marked data are plotted so as to better display the significant differences between the data sets. The D_q values of data set No. 3 and the Lorenz model differ by only about 3%, indicating an excellent agreement between the structure of the laser attractor and the Lorenz attractor. In the case of data set No. 5 the emission of the ring laser in the opposite direction leads to significantly higher D_q values.

Consequently the emission shown in Fig. 1(c) involves, at least at certain times, two laser modes. Thus this pulsing results from a system with a larger phase space than the Lorenz model.

Although the pulsing pattern of Fig. 1(c) does not obviously show the complicated structure which one might expect from a higher-dimensional system like the two-mode laser [6], it is remarkable that the dimension spectrum gives a clear indication of a more complicated attractor.

Additionally, from Fig. 5, it is worth noting that the correlation dimension D_2, commonly used to compare chaotic attractors, appears to be quite insensitive to the attractor dimension and is thus least well suited for characterizing chaotic systems.

We acknowledge the valuable numerical assistance of N. Nafah visiting from the Ecole Polytechnique de Lausanne, Switzerland.

[1] (a) E. N. Lorenz, J. Atmos. Sci. **20**, 130 (1963); (b) H. Haken, Phys. Lett. **53A**, 77 (1975).

[2] U. Hübner, N. B. Abraham, and C. O. Weiss, Phys. Rev. A **40**, 6354 (1989).

[3] H. G. E. Hentschel and I. Procaccia, Physica D **8**, 435 (1983).

[4] K. Pawelzik and H. G. Schuster, Phys. Rev. A **35**, 481 (1987).

[5] P. Grassberger and I. Procaccia, Phys. Rev. Lett. **50**, 346 (1983).

[6] D. Y. Tang, C. O. Weiss, E. Roldan, and G. F. deValcarcel, Opt. Commun. (to be published).